Two Distinct Pathways for Targeting Proteins from the Cytoplasm to the Vacuole/Lysosome

Misuzu Baba,*‡ Masako Osumi,‡ Sidney V. Scott,§ Daniel J. Klionsky,§ and Yoshinori Ohsumi*

*Department of Cell Biology, National Institute for Basic Biology, Okazaki 444, Japan; ‡Department of Chemical and Biological Sciences, Faculty of Science, Japan Women's University, Mejirodai, Tokyo 112, Japan; and §Section of Microbiology, University of California, Davis, California 95616

Abstract. Stress conditions lead to a variety of physiological responses at the cellular level. Autophagy is an essential process used by animal, plant, and fungal cells that allows for both recycling of macromolecular constituents under conditions of nutrient limitation and remodeling the intracellular structure for cell differentiation. To elucidate the molecular basis of autophagic protein transport to the vacuole/lysosome, we have undertaken a morphological and biochemical analysis of this pathway in yeast.

Using the vacuolar hydrolase aminopeptidase I (API) as a marker, we provide evidence that the autophagic pathway overlaps with the biosynthetic pathway, cytoplasm to vacuole targeting (Cvt), used for API import. Before targeting, the precursor form of API is localized mostly in restricted regions of the cytosol as a complex with spherical particles (termed Cvt complex). During vegetative growth, the Cvt complex is selectively wrapped by a membrane sac forming a double membrane-bound structure of ~150 nm diam, which then fuses with the vacuolar membrane. This process is topologically the same as macroautophagy induced under starvation conditions in yeast (Baba, M., K. Takeshige, N. Baba, and Y. Ohsumi. 1994. *J. Cell Biol.* 124:903–913). However, in contrast with autophagy, API import proceeds constitutively in growing conditions. This is the first demonstration of the use of an autophagy-like mechanism for biosynthetic delivery of a vacuolar hydrolase. Another important finding is that when cells are subjected to starvation conditions, the Cvt complex is now taken up by an autophagosome that is much larger and contains other cytosolic components; depending on environmental conditions, the cell uses an alternate pathway to sequester the Cvt complex and selectively deliver API to the vacuole. Together these results indicate that two related but distinct autophagy-like processes are involved in both biogenesis of vacuolar resident proteins and sequestration of substrates to be degraded.

THE vacuole/lysosome is the most dynamic organelle in eukaryotic cells. It is integrally involved in numerous physiological functions (Klionsky et al., 1990) and uses multiple targeting pathways for the delivery of resident hydrolases and degradative substrates (Raymond et al., 1992; Stack et al., 1995; Klionsky, 1997). While in the yeast *Saccharomyces cerevisiae* most vacuolar enzymes reach the organelle through the secretory pathway, two hydrolases, aminopeptidase I (API,[1] encoded by *APE1*; Klionsky et al., 1992) and α-mannosidase (encoded by *AMS1*; Yoshihisa and Anraku, 1990) are known to be transported directly from the cytosol to the vacuole via a *SEC*-independent pathway(s).

The vacuole/lysosome is the terminal destination for much membrane-mediated transport within the cell. The extracellular space is connected with vacuoles/lysosomes by endocytic trafficking, and materials in the environment that are destined for degradation are taken into the lytic compartment by endocytosis or by heterophagy. Plasma membrane proteins such as transporters (Volland et al., 1994) and receptors (Hicke and Riezman, 1996) are delivered to the vacuoles to be degraded as occasion demands.

Under conditions of nutrient stress, it becomes necessary for the cell to degrade cytosolic macromolecules. Cytosolic components are delivered to the vacuole/lysosome by an autophagic process. Autophagy is a major route for vacuolar/lysosomal degradation and is induced by various starvation conditions. This process is accompanied by

Address all correspondence to Yoshinori Ohsumi, Department of Cell Biology, National Institute for Basic Biology, Okazaki 444, Japan. Tel.: (81) 564-55-7515. Fax: (81) 564-55-7516. E-mail: yohsumi@nibb.ac.jp

1. *Abbreviation used in this paper*: API, aminopeptidase I.

quite dynamic membrane rearrangement (Dunn, 1994). When cells recognize depletion of nutrients, a specialized membrane sac, called the isolation membrane, starts to enclose a portion of the cytoplasm and forms a double membrane-bound structure, the autophagosome. The outer membrane of this structure then fuses with a vacuole/lysosome to become an autophagolysosome. In the case of yeast, inner membrane-bound structures (autophagic bodies) appear in the vacuole (Takeshige et al., 1992). If proteinase activity is blocked, the autophagic bodies accumulate in the vacuoles, although a slow breakdown takes place under growing conditions that is *PEP4* independent. Autophagic bodies in wild-type cells are rapidly disintegrated by hydrolytic enzymes in the vacuoles, allowing their contents to be digested and reused. Morphological and biochemical studies have revealed that active cytoplasmic enzymes and organelles are subjected to degradation nonselectively by autophagy during nutrient starvation (Baba et al., 1994). It has also been reported that selective autophagic degradation of specific enzymes (Chiang and Schekman, 1991; Huang and Chiang, 1997) or organelles (Veenhuis et al., 1983; Tuttle et al., 1993) is induced to eliminate excessive or obstructive material. Although little is known about the mechanism of the selective sequestration, in some cases microautophagy seems to be responsible (Tuttle and Dunn, 1995; Chiang et al., 1996).

We have used yeast as a model system to identify the molecular components involved in the macroautophagic process. Previously, we reported the isolation and characterization of 14 autophagy-defective (*apg*) mutants (Tsukada and Ohsumi, 1993). We have now cloned and sequenced 12 *APG* genes, most of which turned out to be novel and nonessential for vegetative growth but essential for autophagy in yeast (Kametaka et al., 1996; Funakoshi et al., 1997; Matsuura et al., 1997).

Recently Klionsky's group isolated a set of mutants, named *cvt* (cytoplasm to vacuole targeting), defective in API maturation (Harding et al., 1995). Complementation studies reveal that the *cvt* mutants overlap with the *apg* (Scott et al., 1996) mutants and the *aut* (Harding et al., 1996) mutants isolated by Thumm et al. (1994) that are also defective in autophagy. This overlap suggests that autophagy and API transport share common machinery. However, these two events are apparently quite distinct from each other in many respects. Autophagy is nonselective and is induced under various starvation conditions, while API transport is selective and proceeds constitutively under growing conditions. Kinetics of the two pathways are also different: autophagy is induced after a lag period of about 30 min, proceeds slowly, and reaches a plateau (Scott et al., 1996); sequestration of the precursor form of API (proAPI) and proteolytic maturation in the vacuole occur with a half time of ~40 min, and are complete within 2 h (Klionsky et al., 1992).

Here we show the morphological events occurring during the sequestration of proAPI to the vacuole and propose a novel mechanism of protein transport to the lytic compartment. These morphological studies together with biochemical analyses of *cvt* mutants indicate that API is transported to the vacuole via two distinct selective pathways. These two pathways are controlled by an unknown mechanism that senses environmental nutrient conditions.

Materials and Methods

Strains and Media

The *Saccharomyces cerevisiae* strains used in this study were SEY6210 (*MATα leu2-3,112 ura3-52 his3-Δ200 trp1-Δ901 lys2-801 suc2-Δ9 GAL*), THY101 (*ape1Δ*::*LEU2* in SEY6210 background), and TVY1 (*pep4Δ*::*LEU2* in SEY6210 background). The TVY1 and THY101 strains were grown to mid-log phase in a rich medium (YEPD containing 1% yeast extract [Difco, Detroit, MI], 2% peptone [Difco] and 2% glucose) at 30°C. Strain SEY6210 transformed with a plasmid pRC1(2μ *APE1*; Klionsky et al., 1992) was grown to log phase in SD (synthetic minimal medium supplemented with the required amino acids). SD(-N) consisting of 1.7 g/liter of yeast nitrogen base without amino acids, ammonium sulfate, or 2% glucose was used for nitrogen starvation experiments.

Electron Microscopy

The cells were washed once with SD(-N) medium, resuspended in the same medium, and incubated for the indicated times at 30°C. The cells were collected by centrifugation and quickly frozen with liquid propane using a rapid freezing device (KF80; Leica, Vienna, Austria). The freeze-substitution fixation method was carried out as described previously (Baba and Osumi, 1987).

Immunoelectron Microscopy

The preparation of immunoelectron microscopy was done according to the procedures described previously (Baba et al., 1994) with slight modifications. The collected cells were sandwiched between an aluminum and a copper disk and quickly frozen as described above. Cells attached to an aluminum disk were transferred to 0.1% formaldehyde in cold-absolute acetone kept below −80°C. Substitution fixation was carried out at −80°C for 1 or 2 d. The specimens were transferred to −20°C and kept for 2 h, washed once with cold absolute acetone, and then replaced stepwise to cold-absolute ethanol at −20°C. Samples were infiltrated with LR White resin (London Resin, Hampshire, UK) at −20°C. The resin was polymerized at −20°C for 48 h under ultraviolet irradiation. Ultrathin sections were collected onto formvar-coated nickel grids. The grids were blocked in 2% BSA-PBS containing chromatographically purified normal goat serum (1:50 dilution) for 30 min at room temperature. API was immunolabeled with affinity-purified API antibody (Klionsky et al., 1992). Incubations were carried out by floating grids on a 20 μl drop of the antibody against API (1:200 or 1:500 dilution) for 1 h at room temperature. After washing, the grids were incubated for 1 h with 10-nm gold–conjugated goat anti–rabbit IgG (Bio Cell Lab., Cardiff, UK). The grids were washed several times in PBS followed by several drops of distilled water and fixed with 1% glutaraldehyde for 3 min. The sections were stained with 4% uranyl acetate for 7 min or further stained with 0.2% lead citrate for 30 s. In all experiments, omission of the primary antiserum resulted in no detectable immunogold particles. Ultrathin sections were examined with an electron microscope (H-800; Hitachi Scientific Instr., Mountain View, CA) at 125 kV.

Pulse–Chase Analysis and Immunoprecipitation

Immunoblotting was performed as described previously (Harding et al., 1996). Cells were grown in SD to 1 OD_{600} U/ml, harvested, washed, and transferred to SD(-N) for 4 h. Pulse–chase conditions and immunoprecipitation were as described (Scott et al., 1996).

Results

ProAPI Assembles into a Cytosolic Complex

API is synthesized as a cytosolic precursor that is targeted to the vacuole independent of the secretory pathway (Klionsky et al., 1992). The molecular basis of the targeting process, however, is not understood. To elucidate the mechanism of API transport to the vacuole, morphological studies were performed using immunoelectron microscopy with specific antibodies against API (Klionsky et al.,

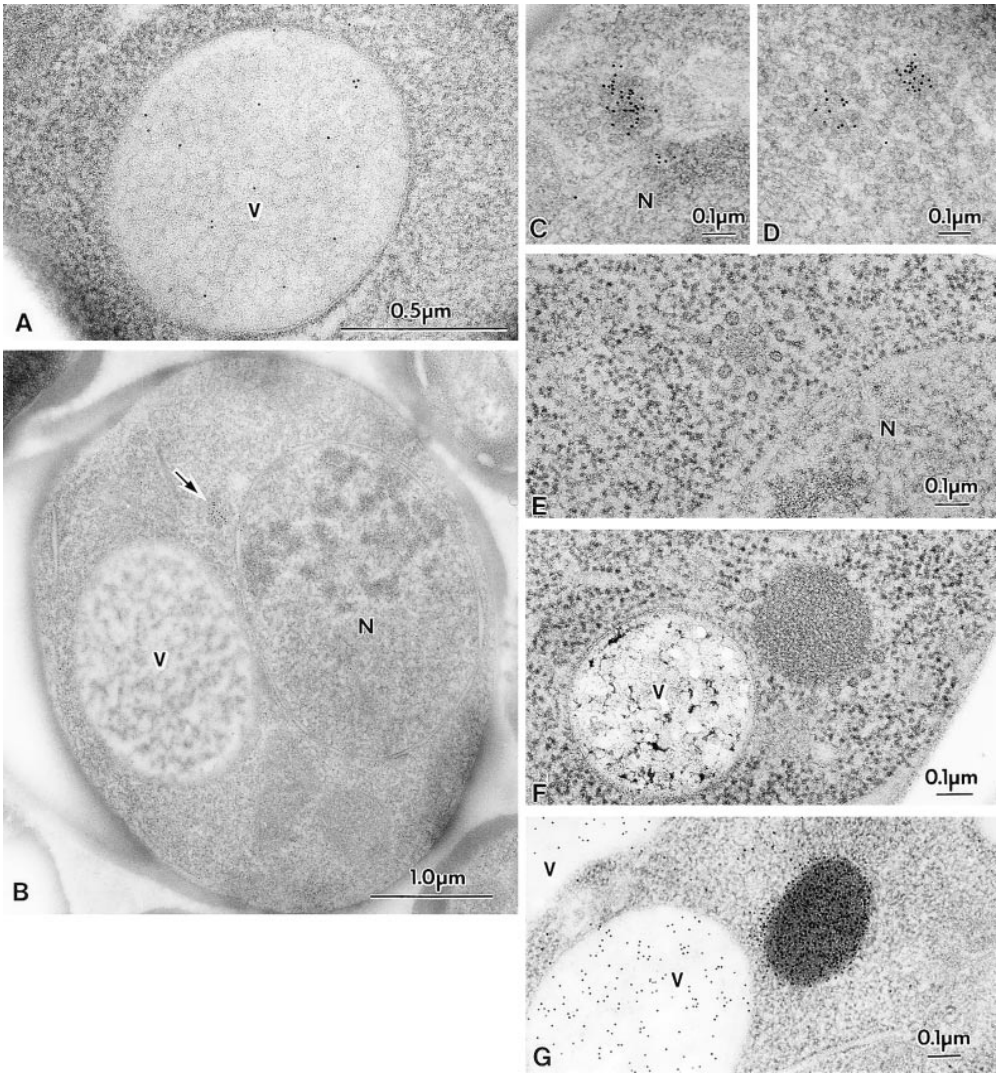

Figure 1. Morphological studies of proAPI in the cytosol. Cells were grown in YEPD medium at 30°C to log phase and were prepared for electron microscopy as described in Materials and Methods. Where indicated, immunostaining of API was performed using antibody to the mature protein that detects both the mature and precursor forms of the hydrolase. (*A*) Immunostaining of API in the vacuole of SEY6210 (wild-type) cell showing a dispersed pattern. (*B–D*) Immunostaining of TVY1 (*pep4*) cells showing API in the Cvt complex. The arrow points to a Cvt complex. Higher magnification images are shown in *C* and *D*. (*E*) Freeze-substitution fixation image of Cvt complex in TVY1 cell. (*F*) Freeze-substitution fixation image of a Cvt complex in strain SEY6210 transformed with a 2μ plasmid encoding API grown in SD medium. (*G*) Immunostaining of strain SEY6210 containing a 2μ *APE1* plasmid grown in SD medium. *N*, Nucleus; *V*, vacuole.

1992). Wild-type or *pep4* mutant cells grown in a rich medium (YEPD) to log phase were examined. API was mostly distributed uniformly in the vacuole (Fig. 1, *A* and *G*), suggesting it is a typical soluble vacuolar enzyme. Its density differed in each vacuole even within a single cell, probably reflecting overall heterogeneity of distribution. In contrast to the dispersed staining pattern seen in the vacuole with the mature enzyme and the expected distribution for a cytosolic enzyme, immunogold particles detecting proAPI were localized in discrete regions of the cytosol (Fig. 1 *B*, *arrow*). Nearly all gold particles were found in large complexes (Fig. 1, *B–D*), while the remaining cytosolic regions contained few proAPI signals. The proAPI clusters were often found near the nucleus (Fig. 1, *B* and *C*). Recent studies indicate that immediately after proAPI synthesis, the protein oligomerizes into a dodecameric form and binds to a pelletable fraction (Kim et al., 1997), which is dependent on a signal in the API propeptide (Oda et al., 1996). The cytosolic proAPI complexes detected in these images are representative of higher-order structures of API dodecamers. Whether proAPI dodecamers are specifically targeted to these cytosolic structures or synthesized and assembled in a restricted area of the cytosol is unknown.

Another striking observation is that the proAPI is associated with spherical particles. By rapid freezing and freeze-substitution fixation we detected an electron-dense core structure surrounded by particles in the cytosol (Fig. 1 *E*; hereafter we call this entire structure the Cvt complex). This type of structure was never detected in the *ape1Δ* cells (data not shown). In *APE1* disruptants, these spherical particles were not found clustered in the cytosol; instead, they were distributed singly or in small clusters of a few together. These results clearly indicate that the core of the complex contains proAPI. It is possible, however, that in the absence of API, Cvt complexes exist but are more difficult to identify.

Cells harboring a multicopy plasmid containing the *APE1* gene showed a single or a few large, electron-dense structures in the cytosol (Fig. 1 *F*), which were heavily stained with antibody against mature API (Fig. 1 *G*) or against the propeptide of proAPI. This further indicates the presence of proAPI within the electron-dense material in the complex. The spherical particles were still associated with proAPI as a large complex (Fig. 1 *F*).

The average size of the spherical particles within the Cvt complex that are associated with proAPI was ~35–50 nm diam by the freeze-substitution fixation method we employed.

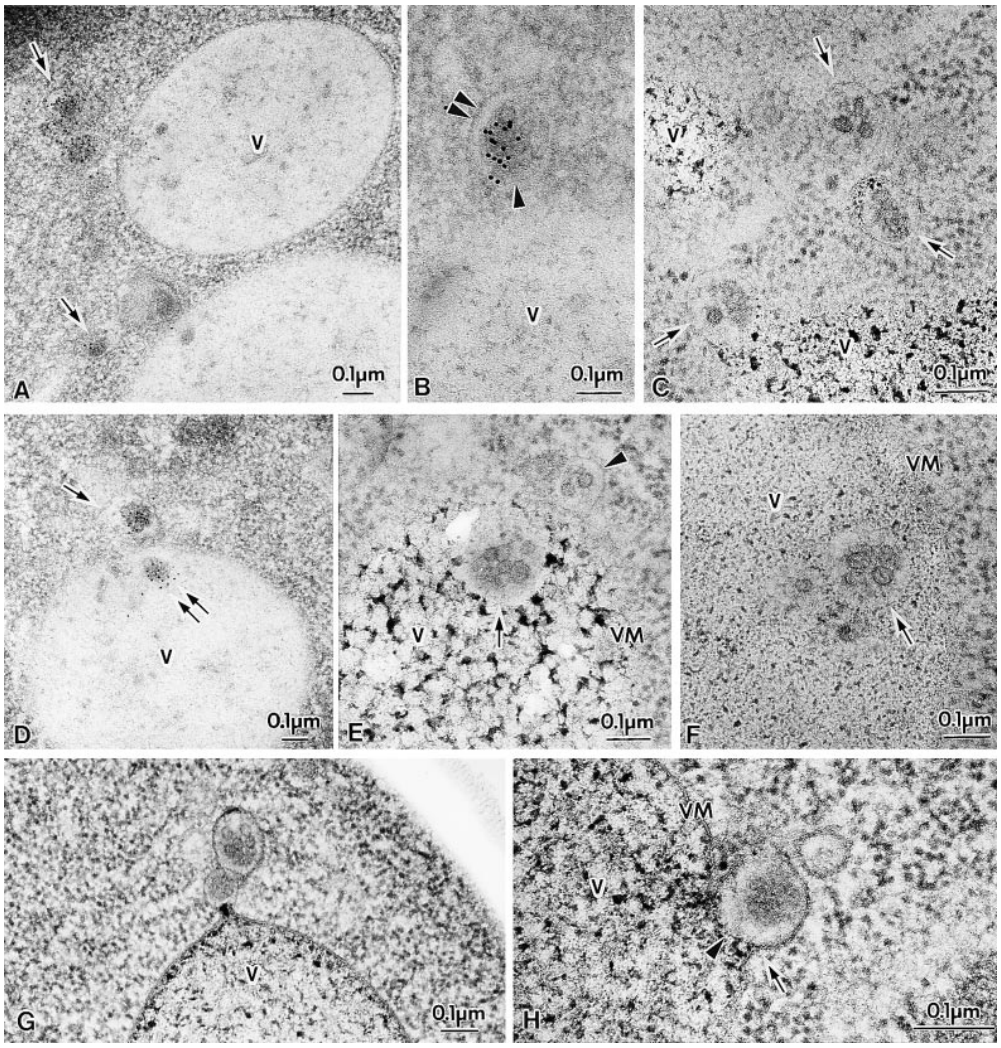

Figure 2. Membrane-bound forms of Cvt complex in TVY1 (*pep4*) cells. Cells were grown in YEPD medium at 30°C to log phase and prepared for electron microscopy as described in Fig. 1. (*A* and *B*) Immunostaining image showing Cvt vesicles (marked with *arrows* in *A*) in the cytosol. Arrowhead and double arrowheads show the inner and outer membrane of Cvt vesicle, respectively. (*C*) Freeze-substitution fixation image of Cvt vesicles (marked with *arrows*). (*D*) Immunostaining of Cvt vesicle (marked with *arrows*) in the cytosol and Cvt body (marked with *double arrows*) in the vacuole. (*E* and *F*) Freeze-substitution fixation image of Cvt bodies in the vacuole (marked with *arrows*). A Cvt vesicle is marked with an arrowhead. (*G* and *H*) Freeze-substitution fixation image of Cvt vesicle contacting and fusing to a vacuole. *V*, Vacuole; *VM*, vacuolar membrane.

Membrane Association of the Cvt Complex

Recently, Segui-Real et al. (1995) proposed a model in which each proAPI molecule inserts into the vacuolar membrane and is translocated directly into the vacuole. However, our present data showed that the cytosolic pool of proAPI resides in complexes and not in a free form. Similarly, the demonstration by Kim et al. (1997) that proAPI forms a cytoplasmic dodecamer and is transported in the oligomeric form argues against direct translocation of individual proAPI molecules. Further analysis revealed that besides being in cytosolic complexes, there is a membrane-enclosed form of proAPI and the associated spherical particles. We refer to this structure as a Cvt vesicle (Fig. 2, *A*, *arrows*, and *B*; see Fig. 7). Most of the Cvt vesicles were located close to the vacuoles. They are double membrane-bound vesicles (Fig. 2, *A* and *B*, *arrowheads*; see Fig. 4, *A–D*), though it was difficult to detect a clear image of unit membrane structure for both the outer and inner membrane similar to those of the yeast autophagosome (Baba et al., 1994, 1995). Based on the electron micrographs, these vesicular structures excluded cytosolic components such as ribosomes and selectively contained the Cvt complex (Fig. 2, *A* and *C*, *arrows*). The size of the Cvt vesicles is fairly homogeneous and calculated to be ~140–160 nm diam, which is a little smaller than the size of the free Cvt complex in the cytosol (Fig. 1 *E*) and also much smaller than the autophagosomes (300–900 nm diam) induced under starvation conditions (Takeshige et al., 1992; Baba et al., 1994). These results are consistent with our previous observation of vesicles found in the cytosol of *cvt17* mutant cells (Scott et al., 1997). As shown later, the ultrastructure of API overproducing cells growing in SD medium supports the above results. We are able to detect a double membrane structure more easily in these cells (Fig. 4, *A–D*).

Novel Pathway of proAPI Transport to the Vacuole

The presence of proAPI in a complex within the vacuole was confirmed by immunoelectron microscopy of *pep4* cells that lack most of the vacuolar enzyme activities (Fig. 2 *D*, *double arrows*). Ultrathin sections of *pep4* cells fixed by freeze-substitution showed the Cvt complex in a membrane-bound form in the vacuole (Fig. 2, *E* and *F*, *arrows*). From examination of many sections, we found evidence for contact (Fig. 2 *G*) and fusion of the Cvt vesicles with the vacuolar membrane (Fig. 2 *H*); the outer membrane of the Cvt vesicle becomes continuous with the vacuolar membrane (Fig. 2 *H*, *arrow*), and the inner membrane faces the vacuole lumen (Fig. 2 *H*, *arrowhead*). These re-

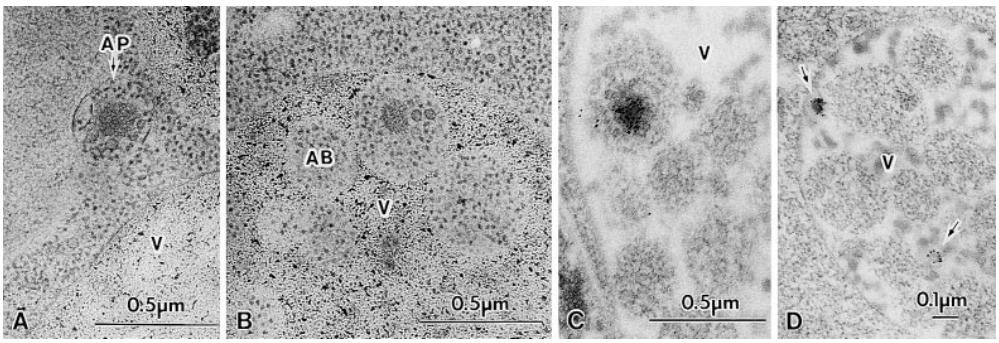

Figure 3. Cvt complexes in TVY1 (*pep4*) cells under nitrogen starvation conditions. Logarithmically growing cells in YEPD were transferred to nitrogen starvation medium (SD[-N]) at 30°C for 30 min (*A* and *B*) or 60 min (*C* and *D*) and prepared for electron microscopy as described in Fig. 1. (*A*) Freeze-substitution fixation image showing a Cvt complex in an autophagosome (marked by an *arrow*) in the cytosol. (*B*) Freeze-substitution fixation image showing a Cvt complex in an autophagic body in the vacuole. (*C*) Immunostaining of a Cvt complex in an autophagic body in the vacuole. (*D*) Immunostaining of Cvt vesicles (marked with *arrows*) in the vacuole. *AB*, Autophagic body; *AP*, autophagosome; *V*, vacuole.

sults strongly suggest Cvt vesicles fuse with the vacuolar membrane and deliver the inner vesicle, which we term Cvt body, into the vacuole lumen. The Cvt bodies correspond to, but are much smaller than, the autophagic bodies that are formed in the process of autophagy and must be the final membrane structure that delivers the Cvt complex to the vacuole.

A single membrane-bound Cvt body could also arise through direct uptake of a Cvt complex at the vacuole surface. However, we never observed an invagination of vacuolar membrane engulfing a Cvt complex, as would occur in microautophagy. Furthermore the membrane of the subvacuolar Cvt body is thin and clearly distinguishable from the vacuolar membrane, which appears as a nicely symmetrical unit membrane. These results strongly suggest that proAPI is delivered to the vacuole via a vesicle-mediated process that is topologically similar to macroautophagy. This may explain the reason why all *APG* genes are required for sequestration and maturation of API in the vacuole (Scott et al., 1996).

Autophagic Mode of API Transport to the Vacuole

It is known that API transport occurs under growing conditions in rich medium. When API is overproduced by a multicopy plasmid during vegetative growth, however, proAPI accumulates, suggesting saturation of a limiting component (Klionsky et al., 1992). Though expression of API is induced 19-fold by starvation, precursor forms do not accumulate under starvation conditions (Scott et al., 1996). These results indicate that the capacity for sequestration of proAPI increases drastically upon starvation (Scott et al., 1996).

To investigate the effect of nitrogen starvation on API transport, *pep4* cells were examined after shift to starvation medium. In contrast to nutrient-rich conditions, we found that the Cvt complexes were now taken up within autophagosomes together with other cytosolic components such as ribosomes (Fig. 3 *A*). When the cells were transferred to nitrogen-starvation medium (SD[-N]) for 30 min or longer, most of the Cvt complex stained with anti-API antibody was found in the autophagic bodies in the vacuoles (Fig. 3, *B* and *C*). Though we demonstrated previously that many cytosolic enzymes are taken up to the vacuole nonselectively (Takeshige et al., 1992; Baba et al., 1994), this observation strongly suggests that during starvation the Cvt complex is preferentially sequestered to the vacuoles via autophagosomes. In the 3-h starved *pep4* cells, Cvt bodies were detected much less frequently than autophagic bodies containing API (Fig. 3 *D*). Among 131 vacuoles containing autophagic bodies, we could observe 18 autophagic bodies containing a Cvt complex inside but could see only two Cvt bodies. Obviously two kinds of membrane structures are responsible for API transport. One is small, contains only the Cvt complex, and functions during vegetative growth; the other is the autophagosome. During starvation, proAPI seems to be transported to the vacuole mostly by the autophagosomes. This explains well the enhanced capacity of sequestration of proAPI under starvation. At this moment it remains to be solved how nutrient conditions control these two processes and whether the Cvt pathway is down regulated under starvation conditions.

Sequestration of Overproduced proAPI

In cells overproducing API from a 2μ plasmid, proAPI forms complexes with the spherical particles that are apparently larger than the size of the Cvt complexes found in cells with chromosomal levels of API (Fig. 1, *F* and *G*). Some of them are much larger than the Cvt vesicles in wild-type cells. We examined these structures more carefully by electron microscopy under both vegetative and starvation conditions. In API overproducing cells grown in SD medium, some of the smaller sized Cvt complexes were enclosed by a double membrane (Fig. 4, *A–D*). Most Cvt vesicles in the API overproducer were 150–250 nm diam. However, every large Cvt complex lacks surrounding membrane. These vesicular structures have clear intermembrane space (Fig. 4, *A* and *C*), indicating that they are double membrane–bound structures. Fig. 4 *E* shows a membrane sac enclosing a small portion of a large Cvt complex, presumably reflecting an intermediate step in formation of a Cvt vesicle.

Cells overproducing API were shifted to nitrogen starvation medium and observed by electron microscopy. Under growing conditions the Cvt complex may become enlarged because synthesis exceeds the capacity of targeting to the vacuole. When cells were examined after a short period after shift to starvation medium, some sections

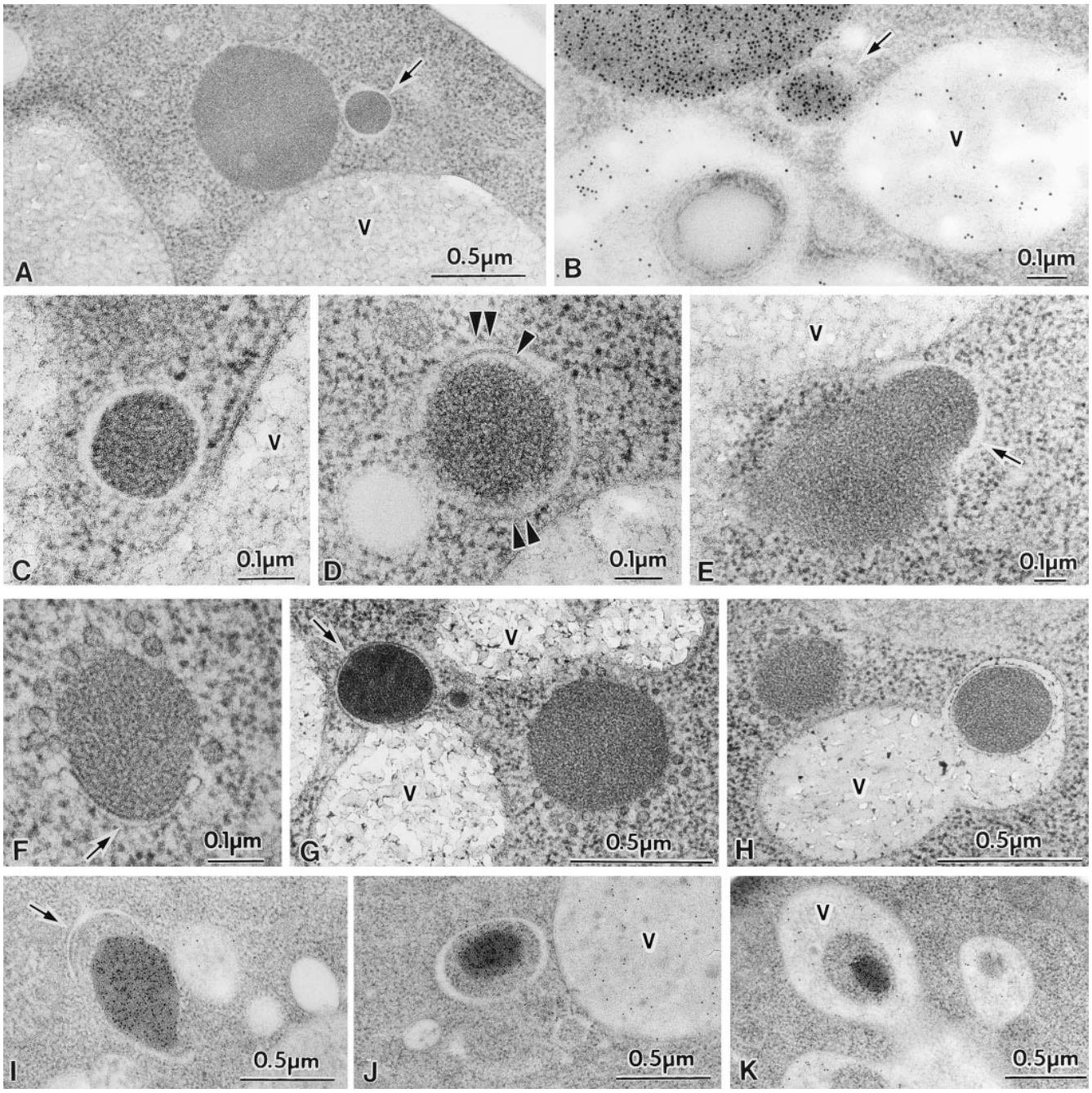

Figure 4. Transport of Cvt complex in SEY6210 (wild-type) harboring 2μ plasmid encoding API under growing and nitrogen starvation conditions. Vegetative cells grown in SD medium were observed (*A–E*). For starvation, logarithmically growing cells in SD were transferred to SD(-N) for 25 min (*F–H*) or 1 h (*I–K*) in the presence of 1 mM PMSF. Samples were prepared for electron microscopy as described in Fig. 1. (*A*) Freeze-substitution fixation image of Cvt vesicle (marked with an *arrow*). (*B*) Immunostaining of a Cvt vesicle (marked with an *arrow*). (*C* and *D*) Higher magnification image of Cvt vesicle. Arrowhead and double arrowheads show the inner and outer membrane of a Cvt vesicle, respectively. (*E*) Freeze-substitution fixation image of a membrane sac enclosing small portion of a large Cvt complex (marked with an *arrow*). (*F*) Freeze-substitution image of the wrapping of a Cvt complex by the isolation membrane (marked with an *arrow*). (*G*) Freeze-substitution image of a Cvt vesicle (marked with an *arrow*) fusing to a vacuole. (*H*) Freeze-substitution image of autophagic body containing a Cvt complex. (*I*) Immunostaining image depicting the wrapping of a Cvt complex. The arrow marks the enwrapping membrane. (*J*) Immunostaining of an autophagosome containing a Cvt complex. (*K*) Immunostaining of an autophagic body containing a Cvt complex in the vacuole. *V*, vacuole.

showed the large complex of proAPI and the associated particles in the process of being enclosed entirely by the isolation membrane (Fig. 4 *F*). The morphology of this enwrapping membrane is quite similar to the isolation membrane involved in the process of autophagy in mammalian cells. Fig. 4 *G* shows one large Cvt complex completely surrounded by a membrane structure and in contact with the vacuole (indicated by an *arrow*) and one unenclosed Cvt

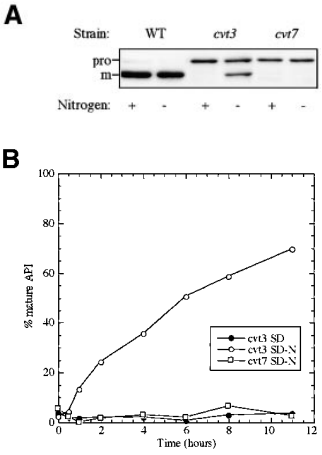

Figure 5. Mutant analysis allows for differentiation between vacuolar delivery by Cvt vesicles and autophagosomes. (*A*) SEY6210 (wild-type), *cvt3*, and *cvt7* yeast were grown in SD to 1 OD_{600} U/ml and transferred to SD (-N). Aliquots were collected after 0 h (+) and 4 h (−) incubation and subjected to immunoblotting. The positions of precursor (*pro*) and mature (*m*) API are indicated. (*B*) *cvt3* and *cvt7* cells were pulse labeled for 10 min. After addition of cold cysteine and methionine, the cells were harvested, washed, and resuspended in either SD or SD(-N) and chased for the indicated times. API was recovered by immunoprecipitation, resolved on SDS polyacrylamide gels, and quantified using a phosphorimager (STORM; Molecular Dynamics, Sunnyvale, CA).

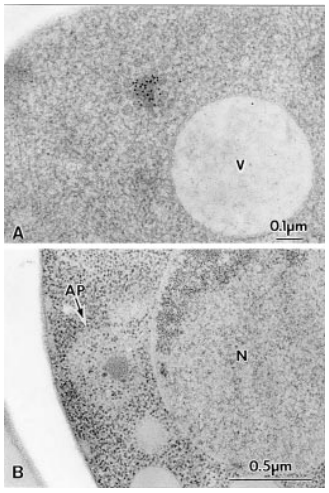

Figure 6. Analysis of the Cvt complex in the *cvt3* mutant under vegetative and starvation conditions. Vegetative cells were grown in SD medium at 30°C to log phase. For starvation, logarithmically growing cells in SD medium were transferred to SD(-N) for 5 h. Samples were prepared for electron microscopy as described in Fig. 1. (*A*) Immunostaining image depicting Cvt complex in the cytosol. Cvt vesicles are not detected in this strain. (*B*) Freeze-substitution fixation image showing Cvt complex in autophagosome (marked with an *arrow*) under starvation conditions, indicating that autophagy can still proceed. *AP*, Autophagosome; *N*, nucleus; *V*, vacuole.

complex. We only observed the enclosed form of these large Cvt complexes under starvation conditions (compare Figs. 4 *A* and 1, *F* and *G*). We detected many membrane-bound forms of Cvt complexes >450 nm diam under these conditions. Large Cvt complexes were also detected in the vacuole during starvation, and while some were surrounded by a membrane (Fig. 4 *H*), most were apparently undergoing transient stages of dissociation. Due to the larger size of the Cvt complexes upon API overproduction, they appeared to be taken up into the autophagosome without cytosol. However, after longer incubation in starvation medium, the size of Cvt complexes decreased, perhaps reflecting a reduced cytosolic pool of precursor API. The smaller Cvt complexes were then enwrapped along with surrounding cytosol (Fig. 4 *I*, *arrow*), as occurs with an autophagosome (Fig. 4 *J*), and are also found in autophagic bodies within the vacuole (Fig. 4 *K*). Uptake of overproduced proAPI by autophagosomes may explain why the capacity for API transport to the vacuole increases under starvation conditions. Even during autophagic uptake, however, API import is rapid, suggesting that it remains a selective, receptor-mediated process.

Two Pathways Are Supported by a Biochemical Analysis of cvt Mutants

The *cvt* mutants, defective in API transport, were identified by screening cells grown in nutrient-rich conditions (Harding et al., 1995; Scott et al., 1996). To determine if the Cvt pathway and autophagy can be distinguished phenotypically, we examined the effect of nitrogen starvation on API transport in these mutants. The *cvt3* and *cvt7*/*apg9*/*aut9* strains are both defective for API import (Harding et al., 1995). However, while *cvt7* is starvation sensitive, *cvt3* is relatively resistant to starvation (Scott et al., 1996). Cells were grown to log phase in nitrogen-containing medium, harvested, and transferred to SD(-N) for 4 h, and cell extracts were examined by Western blot with antibody against API. We found that while both *cvt3* and *cvt7* appeared completely defective in API transport in rich medium, after transfer to nitrogen starvation medium the *cvt3* phenotype was reversed (Fig. 5 *A*). Further, we examined the mutant strains kinetically by pulse-chase analysis. After pulse labeling in nitrogen-containing medium for 10 min, the cells were washed and resuspended in medium either containing or lacking nitrogen. Samples were collected and subjected to immunoprecipitation with anti-mature API antibody. When the chase reaction was carried out in the presence of nitrogen, API transport was completely prevented in both the *cvt3* and *cvt7* cells (Harding et al., 1995). However, on shifting to nitrogen-starvation medium, the cells recovered from the *cvt3* defect, but not the *cvt7* defect (Fig. 5 *B*).

Electron microscopic analysis of *cvt3* mutant cells grown in rich medium revealed that Cvt complexes were present in the cytosol (Fig. 6 *A*). Among 561 cells examined, 43 Cvt complexes were observed in the cytosol, but none of them were surrounded by membrane. When *cvt3* cells were placed under starvation conditions for 1 h, many Cvt complexes were present, but no Cvt vesicles were detected. In contrast, after long incubation in SD(-N) we could see autophagosomes (Fig. 6 *B*) and autophagic bodies containing Cvt complexes. Induction of autophagy may be slower in the *cvt3* mutant compared to wild-type, and the resulting autophagosomes appear to be slightly aberrant. These results support our biochemical analysis and suggest that the *CVT3* gene encodes a molecule that is essential for the Cvt pathway but not for autophagy; under starvation conditions, API can be transported by autophagy, even though the Cvt pathway is defective. In contrast, *CVT7*/*APG9* is necessary for both pathways. In addition, the observation that the transport of API approaches completion in *cvt3* under starvation conditions suggests that a selective autophagic mechanism is used; nonselective transport of cytosolic protein such as Pho8Δ60p by autophagy appears to plateau at ~30% import (Scott et al., 1996). This fact again indicates that sequestration of the Cvt complex by the autophagosome is a selective process. The finding that the *cvt3* mutant is defective for the Cvt pathway but not

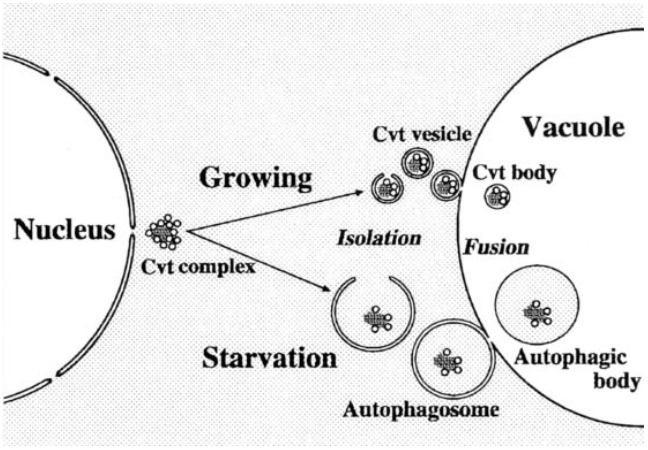

Figure 7. Scheme of API transport pathways to the vacuole. As described in the text, proAPI forms a complex in the cytosol. This Cvt complex is then targeted to the vacuole by two pathways depending upon the nutrient conditions. In growing conditions, a double membrane vesicle of ~140 to 160 nm forms around the Cvt complex and excludes cytosol. In contrast, when cells are starved for nitrogen, the Cvt complex is taken up into larger autophagosomes (300–900 nm) together with cytosolic components. Vacuolar delivery is achieved by fusion of the outer membrane of the Cvt vesicle or autophagosome with the vacuolar membrane. Finally, the resulting Cvt bodies or autophagic bodies are broken down by vacuolar hydrolases to release proAPI into the vacuole lumen. The precursor form of the protein is then processed into the mature hydrolase.

autophagy provides independent support for the idea that two separate but related pathways are responsible for targeting API to the vacuole.

Discussion

Here we presented morphological and biochemical lines of evidence for two pathways used to target API to the vacuole (Fig. 7). A novel pathway under growing conditions consists of selective isolation of specific molecules from the cytosol, targeting, and fusion of the resulting vesicles (Cvt vesicles) with the vacuolar membrane. These findings raise one obvious question: what is the signal for this selective sequestration to the vacuole? The complex of proAPI and the particles may have a specific signal for initiation of formation of the isolation membrane. One possibility is that an individual proAPI protein has a unique signal for selective wrapping by the specialized membrane. A second possibility is that the proAPI protein has a signal for the formation of a complex, and the complex form of proAPI then presents a signal for the wrapping. While the propeptide region of proAPI is necessary for proper targeting of proAPI to the vacuole (Oda et al., 1996), other domains of the protein may be involved in oligomer and/or complex formation. Analysis of API mutants by electron microscopy may provide clear answers to the above possibilities. Thirdly, it is also possible that wrapping is signaled by the spherical particles in the complex or another unidentified component.

The use of common machinery for two seemingly opposite pathways (one biosynthetic and the other degradative) may reflect the need for conservation of cellular resources. The novel Cvt pathway functions in the biogenesis of a vacuolar resident hydrolase, API. It is possible that additional vacuolar resident proteins including α-mannosidase (Yoshihisa and Anraku, 1990) are also transported by this mechanism. However, so far we have not been able to detect α-mannosidase by immunostaining.

The origin of the Cvt pathway and many proteins involved in this transport process are not identified. It would seem wasteful for the cell to develop a completely novel pathway for targeting a limited number of hydrolases to the vacuole. Alternatively, the mechanism involved in API biogenesis may use the preexisting autophagic machinery for delivery to the lytic compartment. The genetic and phenotypic overlap between *cvt* and *apg* mutants suggests that the machinery used by both pathways is largely the same, with the possible exception of receptors and/or other components that allow API uptake to be rapid and specific. Starvation conditions may result in a dynamic membrane mobilization for sequestering a large amount of cytosolic components to the vacuole. The molecular basis of this shift, however, remains to be determined.

Recently, fructose1,6-bisphosphatase has been shown to be degraded in the vacuoles by a vesicle-mediated process. Huang and Chiang (1997) obtained *vid* mutants defective in this process. Although both the Cvt and Vid pathways mediate the delivery of specific polypeptides from the cytosol to the vacuole, there are probably only limited similarities between them. First, the Cvt pathway is constitutive, and autophagy occurs upon starvation (e.g., glucose deprivation). In contrast, the Vid pathway is induced upon glucose addition to starved cells, the opposite conditions for induction of autophagy. Second, the Vid-vesicles are 30–40 nm diam, while Cvt vesicles and autophagosomes are 140–160 and 300–900 nm, respectively. Further information about these processes including any potential overlap will be revealed as we begin to identify the molecular components involved in cytoplasm to vacuole delivery pathways. This study provided the first morphological evidence for selective vesicle-mediated targeting pathways of a resident protein from the cytosol to the lysosome/vacuole.

We are grateful to Dr. M. Filosa for critical reading of the manuscript.

This work was supported in part by Grants-in-Aid for Scientific Research from the Ministry of Education, Science, and Culture of Japan, and Special Coordination Funds for the Promotion of Science and Technology from the Science and Technology Agency of Japan.

Received for publication 27 May 1997 and in revised form 8 September 1997.

References

Baba, M., and M. Osumi. 1987. Transmission and scanning electron microscopic examination of intracellular organelles in Freeze-substituted *Kloeckera* and *Saccharomyces cerevisiae* yeast cells. *J. Electron Microsc. Techn.* 5:249–261.

Baba, M., K. Takeshige, N. Baba, and Y. Ohsumi. 1994. Ultrastructural analysis of the autophagic process in yeast: detection of autophagosomes and their characterization. *J. Cell Biol.* 124:903–913.

Baba, M., M. Osumi, and Y. Ohsumi. 1995. Analysis of the membrane structures involved in autophagy in yeast by freeze-replica method. *Cell Struct. Funct.* 20:465–472.

Chiang, H.-L., and R. Schekman. 1991. Regulated import and degradation of a cytosolic protein in the yeast vacuole. *Nature.* 350:313–318.

Chiang, H.-L., R. Schekman, and S. Hamamoto. 1996. Selective uptake of cytosolic, peroxisomal, and plasma membrane proteins into the yeast lysosome for degradation. *J. Biol. Chem.* 271:9934–9941.

Dunn, W.A., Jr. 1994. Autophagy and related mechanisms of lysosome-medi-

ated protein degradation. *Trends Cell Biol.* 4:139–143.
Funakoshi, T., A. Matsuura, T. Noda, and Y. Ohsumi. 1997. Analyses of *APG13* gene involved in the autophagy in yeast, *Saccharomyces cerevisiae. Gene.* 192:207–213.
Harding, T.M., K.A. Morano, S.V. Scott, and D.J. Klionsky. 1995. Isolation and characterization of yeast mutants in the cytoplasm to vacuole protein targeting pathway. *J. Cell Biol.* 131:591–602.
Harding, T.M., A. Hefner-Gravink, M. Thumm, and D.J. Klionsky. 1996. Genetic and phenotypic overlap between autophagy and the cytoplasm to vacuole protein targeting pathway. *J. Biol. Chem.* 271:17621–17624.
Hicke, L., and H. Riezman. 1996. Ubiquitination of a yeast plasma membrane receptor signals for its ligand-stimulated endocytosis. *Cell.* 84:277–287.
Huang, P.-H., and H.-L. Chiang. 1997. Identification of novel vesicles in the cytosol to vacuole protein degradation pathway. *J. Cell Biol.* 136:803–810.
Kametaka, S., A. Matsuura, Y. Wada, and Y. Ohsumi. 1996. Structural and functional analyses of *APG5*, a gene involved in autophagy in yeast. *Gene.* 178:139–143.
Kim, J., S.V. Scott, M. Oda, and D.J. Klionsky. 1997. Transport of a large oligomeric protein by the cytoplam to vacuole protein targeting pathway. *J. Cell Biol.* 137:609–618.
Klionsky, D.J. 1997. Protein transport from the cytoplasm into the vacuole. *J. Membr. Biol.* 157:105–115.
Klionsky, D.J., P.K. Herman, and S.D. Emr. 1990. The fungal vacuole: composition, function, and biogenesis. *Microbiol. Rev.* 54:266–292.
Klionsky, D.J., R. Cueva, and D.S. Yaver. 1992. Aminopeptidase I of *Saccharomyces cerevisiae* is localized to the vacuole independent of the secretory pathway. *J. Cell Biol.* 119:287–299.
Matsuura, A., M. Tsukada, Y. Wada, and Y. Ohsumi. 1997. Apg1p, a novel protein kinase required for the autophagic process in *Saccharomyces cerevisiae. Gene.* 192:245–250.
Oda, M.N., S.V. Scott, A. Hefner-Gravink., A.D. Caffarelli, and D.J. Klionsky. 1996. Identification of a cytoplasm to vacuole targeting determinant in aminopeptidase I. *J. Cell Biol.* 132:999–1010.
Raymond, C.K., C.J. Roberts, K.E. Moore, I. Howald, and T.H. Stevens. 1992. Biogenesis of the vacuole in *Saccharomyces cerevisiae. Int. Rev. Cytol.* 139: 59–120.
Scott, S.V., A. Hefner-Gravink, A. Morano, T. Noda, Y. Ohsumi, and D.J. Klionsky. 1996. Cytoplasm-to-vacuole targeting and autophagy employ the same machinery to deliver proteins to the yeast vacuole. *Proc. Natl. Acad. Sci. USA.* 93:12304–12308.
Scott, S.V., M. Baba, Y. Ohsumi, and D.J. Klionsky. 1997. Aminopeptidase I is targeted to the vacuole by a nonclassical vesicular mechanism. *J. Cell Biol.* 138:37–44.
Segui-Real, B., M. Martinez, and I.V. Sandoval. 1995. Yeast aminopeptidase I is post-translationally sorted from the cytosol to the vacuole by a mechanism mediated by its bipartite N-terminal extension. *EMBO (Eur. Mol. Biol. Organ.) J.* 14:5476–5484.
Stack, J.H., B. Horazozdovsky, and S.D. Emr. 1995. Receptor-mediated protein sorting to the vacuole in yeast: roles for a protein kinase, a lipid kinase and GTP-binding proteins. *Annu. Rev. Cell Dev. Biol.* 11:1–33.
Takeshige, K., M. Baba, S. Tsuboi, T. Noda, and Y. Ohsumi. 1992. Autophagy in yeast demonstrated with proteinase-deficient mutants and conditions for its induction. *J. Cell Biol.* 119:301–311.
Thumm, M., R. Egner, B. Schlumpberger, M. Straub., M. Veenhuis, and D.H. Wolf. 1994. Isolation of autophagocytosis mutants of *Saccharomyces cerevisiae. FEBS Lett.* 349:275–280.
Tuttle, E.L., and W.A. Dunn, Jr. 1995. Divergent modes of autophagy in the methylotrophic yeast *Pichia pastoris. J. Cell Sci.* 143:212–217.
Tuttle, D.L., A.S. Lewin, and W.A. Dunn, Jr. 1993. Selective autophagy of peroxisomes in methylotrophic yeasts. *Eur. J. Cell Biol.* 60:283–290.
Tsukada, M., and Y. Ohsumi. 1993. Isolation and characterization of autophagy-defective mutants of *Saccharomyces cerevisiae. FEBS Lett.* 333:169–174.
Veenhuis, M., A. Douma, W. Harder, and M. Osumi. 1983. Degradation and turnover of peroxisomes in the yeast *Hansenula polymorpha* induced by selective inactivation of peroxisomal enzymes. *Arch. Microbiol.* 134:193–203.
Volland, C., D. Urban-Grima, G. Geraud, and R. Haguennauer-Tsapis. 1994. Endocytosis and degradation of the yeast uracil permease under adverse conditions. *J. Biol. Chem.* 269:9833–9841.
Yoshihisa, T., and Y. Anraku. 1990. A novel pathway of α-mannosidase, a marker enzyme of vacuolar membrane, in *Saccharomyces cerevisiae. J. Biol. Chem.* 265:22418–22425.